Structural Engineering and Mechanics, *Vol. 61, No. 6 (2017) 807-816*
DOI: https://doi.org/10.12989/sem.2017.61.6.807

Automated static condensation method for local analysis of large finite element models

Seung-Hwan Boo[*1] and Min-Han Oh[2a]

[1]*Department of Mechanical Engineering, Korea Advanced Institute of Science and Technology, 291 Daehak-ro, Yuseong-gu, Daejeon 34141, Republic of Korea*
[2]*Offshore Engineering Research Department, Hyundai Heavy Industries, 1000 Bangeojinsunhwan-doro, Dong-gu, Ulsan 682-792, Republic of Korea*

(Received January 27, 2017, Revised February 26, 2017, Accepted February 27, 2017)

Abstract. In this paper, we introduce an efficient new model reduction method, named the automated static condensation method, which is developed for the local analysis of large finite element models. The algebraic multilevel substructuring procedure is modified appropriately, and then applied to the original static condensation method. The retained substructure, which is the local finite element model to be analyzed, is defined, and then the remaining part of the global model is automatically partitioned into many omitted substructures in an algebraic perspective. For an efficient condensation procedure, a substructural tree diagram and substructural sets are established. Using these, the omitted substructures are sequentially condensed into the retained substructure to construct the reduced model. Using several large practical engineering problems, the performance of the proposed method is demonstrated in terms of its solution accuracy and computational efficiency, compared to the original static condensation method and the superelement technique.

Keywords: finite element model; local analysis; model reduction method; static condensation method; superelement technique; algebraic multilevel substructuring

1. Introduction

For decades, structural analysis using finite element (FE) models has been widely conducted in various engineering fields, and it has played a very important role in structural design. With the recent substantial improvement of computer resources, the demand for structural analysis of large, complex FE models has increased more than ever before.

In general, until the design of a structure is completed, the structural analysis is performed iteratively for several times. Therefore, when local analysis of a region of interest should be required, it is advantageous to construct a reduced model of the local region using a static model reduction method, rather than to perform the analysis iteratively using the entire FE model. For this, the static condensation method (Irons 1963, Guyan 1965, Wilson 1974) and the superelement technique (Jagadish *et al*. 2007, Long *et al*. 2013, MSC Nastran 2014) have frequently been employed to construct the reduced model for the local analysis.

In the static condensation method, the degrees of freedom (DOFs) are divided into the retained and omitted DOFs, and the reduced model is constructed by condensing the physical quantities corresponding to the omitted DOFs, into those of the retained DOFs. The static condensation method has been the cornerstone of several dynamic model reduction methods, such as the improved reduced system (IRS) method (O' Callahan 1989), its iterative methods (Friswell et al. 1995, Xia and Lin 2004), and the component mode synthesis (CMS) methods (Craig and Bampton 1968, MacNeal 1971, Benfield and Hruda 1971, Rubin 1975, Han 2014, Boo *et al*. 2016). The static condensation method provides an exact solution for static analysis, while it gives an approximated solution for dynamic analysis because it ignores the inertial effect of the omitted DOFs.

In the late 1960s, the superelement technique was developed by applying the physical domain-based substructuring scheme to the static condensation method. Thus, the efficiency of the computations needed to construct the reduced model was considerably improved. The superelement technique was embedded in MSC Nastran, ANSYS, and ABAQUS, which are very well known commercial FE analysis programs. These are frequently applied to the static and dynamic analyses of the practical engineering problems (Agrawal *et al*. 1994, Cardona 2000, Ju and Choo 2005).

Considering the recent trend of increased demand for analysis of large FE models, computational efficiency has been regarded as the one of the most important requirements in model reduction methods. To meet this demand, an algebraic multilevel substructuring technique (George 1973, Karypis and Kumar 1998) was successfully adopted in several dynamic model reduction methods (Bennighof and Lehoucq 2004, Boo and Lee 2016). These methods can solve very large FE models (over 10^5 DOFs) with remarkable computational efficiency.

*Corresponding author, Post-doctoral Researcher
E-mail: shboo@kaist.ac.kr
[a]Senior Researcher

ISSN: 1225-4568 (Print), 1598-6217 (Online)

In this study, by applying the algebraic multilevel substructuring technique to the original static condensation method, we develop a new static model reduction method, named the automated static condensation method, for efficient local analysis of large FE models. After permuting the global stiffness matrix and force vector though the algebraic multilevel substructuring, the retained substructure, which is regarded as the local model of interest, is defined through the matrix re-permutation based on the node numbers of the local model.

Then, the omitted substructures are automatically defined in the algebraic perspective. The condensation procedures of the proposed method are illustrated sequentially, and using the substructural sets defined in the substructural tree diagram established, we provide substructural matrices updating that occurs during the condensation procedures. The general formulation of the reduced model is expressed using multiplications and summations of submatrices. Using several large practical engineering problems, we demonstrate the excellent computational efficiency of the proposed method in comparison to the original static condensation method and superelement technique.

In Section 2, the formulation of the original static condensation method is briefly reviewed, and the proposed method is derived in Section 3. The performance of the proposed method is compared to the static condensation method and the superelement technique, in Sections 4 and 5, respectively. Finally, conclusions are drawn in Section 6.

2. Static condensation method

In this section, we briefly review the formulation of the static condensation method (Irons 1963, Guyan 1965, Wilson 1974).

The linear static equation is given by

$$\mathbf{K}_g \mathbf{u}_g = \mathbf{F}_g \tag{1}$$

where $\mathbf{K}_g$ is the global stiffness matrix, and $\mathbf{u}_g$ and $\mathbf{F}_g$ are the global displacement and force vectors, respectively.

In the static condensation method, the linear static equation described in Eq. (1) is partitioned as

$$\begin{bmatrix} \mathbf{K}_o & \mathbf{K}_{or} \\ \mathbf{K}_{or}^T & \mathbf{K}_r \end{bmatrix} \begin{bmatrix} \mathbf{u}_o \\ \mathbf{u}_r \end{bmatrix} = \begin{bmatrix} \mathbf{F}_o \\ \mathbf{F}_r \end{bmatrix} \tag{2}$$

in which the subscripts *o* and *r* denote the omitted and the retained DOFs, respectively, and *or* denotes the coupled DOFs between the omitted and the retained DOFs.

Expanding the 1st row equation in Eq. (2), the omitted displacement vector $\mathbf{u}_o$ is represented as

$$\mathbf{u}_o = \mathbf{\Psi}\mathbf{u}_r + \mathbf{K}_o^{-1}\mathbf{F}_o \quad \text{with} \quad \mathbf{\Psi} = -\mathbf{K}_o^{-1}\mathbf{K}_{or}, \tag{3}$$

where $\mathbf{\Psi}$ denotes the constraint mode matrix (Craig and Bampton 1968) to couple the omitted DOFs with the retained DOFs.

Then, expanding the 2nd row equation in Eq. (2), the following equation is obtained as

$$\mathbf{K}_{or}^T \mathbf{u}_o + \mathbf{K}_r \mathbf{u}_r = \mathbf{F}_r \tag{4}$$

Substituting Eq. (3) into Eq. (4), we can obtain the reduced linear static equation as follows

$$\overline{\mathbf{K}}\mathbf{u}_r = \overline{\mathbf{F}} \quad \text{with} \quad \overline{\mathbf{K}} = \mathbf{K}_r + \mathbf{K}_{or}^T\mathbf{\Psi}, \quad \overline{\mathbf{F}} = \mathbf{F}_r + \mathbf{\Psi}^T\mathbf{F}_o, \tag{5}$$

and finally, the displacement vector for the retained DOFs, $\mathbf{u}_r$, is defined as

$$\mathbf{u}_r = \overline{\mathbf{K}}^{-1}\overline{\mathbf{F}} \tag{6}$$

From Eq. (5), it is identified that we only have to compute the constraint mode matrix $\mathbf{\Psi}$ to obtain the reduced linear static equation. Note that, the constraint mode matrix $\mathbf{\Psi}$ is calculated from the linear solving of $\mathbf{K}_o\mathbf{\Psi} = -\mathbf{K}_{or}$, without direct calculation of the inverse matrix $\mathbf{K}_o^{-1}$. The computational cost for the constraint mode matrix $\mathbf{\Psi}$ occupies most of the total computational cost in the static condensation method.

Although the reduced stiffness matrix $\overline{\mathbf{K}}$ and force vector $\overline{\mathbf{F}}$ described in Eq. (5) are calculated through simple matrix operations, the static condensation method is not appropriate for solving large FE models (over 10^5 DOFs). In large FE models, the number of omitted DOFs is considerably larger, and thus, the computational cost for calculating the constraint mode matrix $\mathbf{\Psi}$ becomes very expensive. This will be proved using numerical examples in Section 4.

3. Automated static condensation method

In this section, we describe the algebraic multilevel substructuring and automated static condensation procedures that are the key procedures of the proposed method.

3.1 Algebraic multilevel substructuring procedure

In the original algebraic multilevel substructuring (Karypis and Kumar 1998), the global matrix, which is a very sparse matrix, is automatically permuted, and partitioned into many submatrices.

Then, those submatrices are defined as substructures in the algebraic perspective, and the substructural tree diagram, which defines the relationships among the substructures, is constructed. The details are well described in Fig. 1.

However, in the original algebraic multilevel substructuring, the stiffness terms for the local model to be analyzed may be scattered in the permuted matrix. Fortunately, because the node numbers of the local model are already known, through the re-permutation of the matrix, the scattered stiffness terms can be gathered intentionally. Then, we can define the retained substructure, which corresponds to the local model to be analyzed. The modified algebraic multilevel substructuring procedure is shown in Fig. 2.

Based on Fig. 2, the partitioned linear static equation in the proposed method is written as

$$\mathbf{K}_g \mathbf{u}_g = \mathbf{F}_g, \tag{7}$$

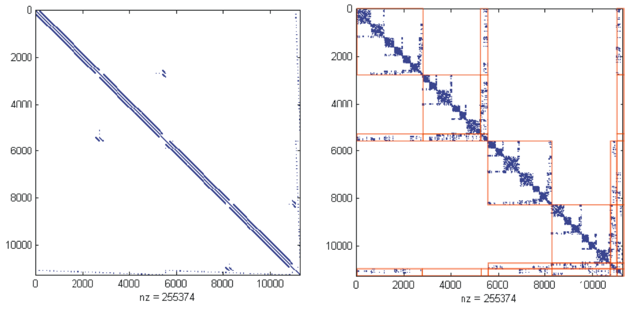

(a) Original large sparse matrix (b) Matrix permutation and partitioning

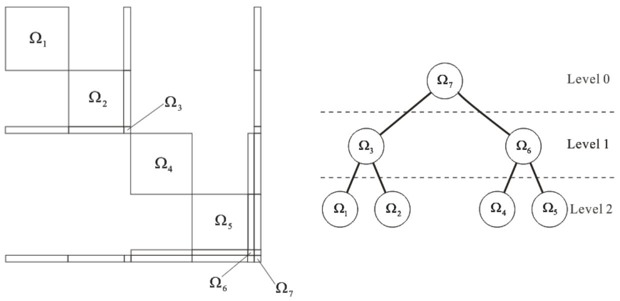

(c) Definition of substructures (d) Definition of substructural tree diagram

Fig. 1 Algebraic multilevel substructuring procedure (seven substructures with two substructural level, where Ω_i denotes the i^{th} substructure)

$$\mathbf{K}_g = \begin{bmatrix} \mathbf{K}_1 & \mathbf{0} & \mathbf{K}_{1,3} & \mathbf{0} & \mathbf{0} & \mathbf{0} & \mathbf{K}_{1,7} & \mathbf{K}_{1,r} \\ & \mathbf{K}_2 & \mathbf{K}_{2,3} & \mathbf{0} & \mathbf{0} & \mathbf{0} & \mathbf{K}_{2,7} & \mathbf{K}_{2,r} \\ & & \mathbf{K}_3 & \mathbf{0} & \mathbf{0} & \mathbf{0} & \mathbf{K}_{3,7} & \mathbf{K}_{3,r} \\ & & & \mathbf{K}_4 & \mathbf{0} & \mathbf{K}_{4,6} & \mathbf{K}_{4,7} & \mathbf{K}_{4,r} \\ & & & & \mathbf{K}_5 & \mathbf{K}_{5,6} & \mathbf{K}_{5,7} & \mathbf{K}_{5,r} \\ & & & & & \mathbf{K}_6 & \mathbf{K}_{6,7} & \mathbf{K}_{6,r} \\ & sym. & & & & & \mathbf{K}_7 & \mathbf{K}_{7,r} \\ & & & & & & & \mathbf{K}_r \end{bmatrix},$$

$$\mathbf{u}_g = \begin{bmatrix} \mathbf{u}_1 \\ \mathbf{u}_2 \\ \mathbf{u}_3 \\ \mathbf{u}_4 \\ \mathbf{u}_5 \\ \mathbf{u}_6 \\ \mathbf{u}_7 \\ \mathbf{u}_r \end{bmatrix}, \quad \mathbf{F}_g = \begin{bmatrix} \mathbf{F}_1 \\ \mathbf{F}_2 \\ \mathbf{F}_3 \\ \mathbf{F}_4 \\ \mathbf{F}_5 \\ \mathbf{F}_6 \\ \mathbf{F}_7 \\ \mathbf{F}_r \end{bmatrix}, \tag{8}$$

where $\mathbf{K}_i$, $\mathbf{u}_i$, and $\mathbf{F}_i$ are the stiffness matrix, displacement vector, and force vector of the i^{th} substructure, respectively. $\mathbf{K}_{i,j}$ is the stiffness matrix of the i^{th} substructure coupled with the j^{th} substructure.

Here, the 1st through 7th substructures become the omitted substructures, and the related quantities corresponding to those substructures will be condensed out. The subscript r denotes the quantities related to the retained substructure to be analyzed.

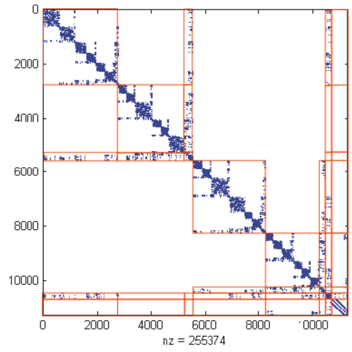

(a) Re-permutated and re-partitioned matrix

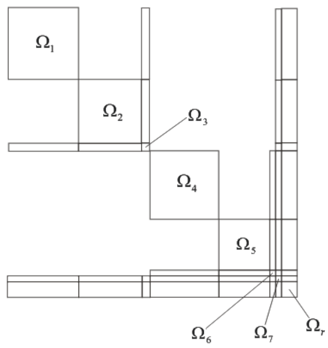

(b) Definition of substructures

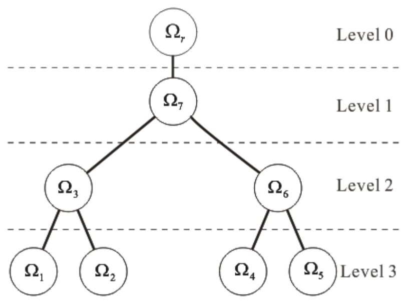

(c) Definition of substructural tree diagram

Fig. 2 Modified algebraic multilevel substructuring procedure (eight substructures with three substructural level, where Ω_r denotes the retained substructure to be analyzed)

Using the substructural tree diagram described in Fig. 2(c), the substructures are categorized into the bottom and higher substructures. Here, the bottom substructures refer to the substructures in the lowest substructural level, and the higher substructures refer to the substructures above the lowest substructural level. In addition, by considering the substructural level to which each substructure belongs, the ancestor substructures for each substructure can be defined.

Let B and H be the sets of the bottom and higher substructures, respectively, and let A_i be the set of ancestor substructures for the i^{th} substructure. Thus, we can define the bottom and higher substructural sets as follows, $B=\{1,2,4,5\}$ and $H=\{3,6,7,r\}$.

The ancestor substructural sets for the 1st, 3rd, and 7th substructures are defined as $A_1=\{3,7,r\}$, $A_3=\{7,r\}$, and $A_7=\{r\}$. The other ancestor substructural sets can be defined in the same manner. Note that the defined substructural sets have an important role to perform for the efficiency of the matrix computations.

3.2 Automated static condensation procedure

Expanding the 1st row equation in Eq. (8), the following equation is obtained

$$\mathbf{K}_1\mathbf{u}_1+\mathbf{K}_{1,3}\mathbf{u}_3+\mathbf{K}_{1,7}\mathbf{u}_7+\mathbf{K}_{1,r}\mathbf{u}_r=\mathbf{F}_1, \tag{9}$$

and the displacement vector $\mathbf{u}_1$ corresponding to the 1st substructure is written by

$$\mathbf{u}_1=\mathbf{\Psi}_{1,3}\mathbf{u}_3+\mathbf{\Psi}_{1,7}\mathbf{u}_7+\mathbf{\Psi}_{1,r}\mathbf{u}_r+\mathbf{K}_1^{-1}\mathbf{F}_1, \tag{10a}$$

$$\mathbf{\Psi}_{1,3}=-\mathbf{K}_1^{-1}\mathbf{K}_{1,3},\quad \mathbf{\Psi}_{1,7}=-\mathbf{K}_1^{-1}\mathbf{K}_{1,7},\quad \mathbf{\Psi}_{1,r}=-\mathbf{K}_1^{-1}\mathbf{K}_{1,r}. \tag{10b}$$

Substituting $\mathbf{u}_1$ in Eq. (10a) into the global displacement vector $\mathbf{u}_g$ in Eq. (8), the following equation is obtained

$$\mathbf{u}_g=\begin{bmatrix}\mathbf{u}_1\\ \hdashline \mathbf{u}_2\\ \mathbf{u}_3\\ \mathbf{u}_4\\ \mathbf{u}_5\\ \mathbf{u}_6\\ \mathbf{u}_7\\ \mathbf{u}_r\end{bmatrix}=\begin{bmatrix}\mathbf{\Psi}_{1,3}\mathbf{u}_3+\mathbf{\Psi}_{1,7}\mathbf{u}_7+\mathbf{\Psi}_{1,r}\mathbf{u}_r+\mathbf{K}_1^{-1}\mathbf{F}_1\\ \hdashline \mathbf{u}_2\\ \mathbf{u}_3\\ \mathbf{u}_4\\ \mathbf{u}_5\\ \mathbf{u}_6\\ \mathbf{u}_7\\ \mathbf{u}_r\end{bmatrix}. \tag{11}$$

From Eq. (11), the global displacement vector $\mathbf{u}_g$ can be rewritten as

$$\mathbf{u}_g=\mathbf{C}_1\mathbf{u}_g^{(1)}+\mathbf{F}_a^{(1)}, \tag{12a}$$

$$\mathbf{C}_1=\left[\begin{array}{c:ccccccc}\mathbf{0} & \mathbf{0} & \mathbf{\Psi}_{1,3} & \mathbf{0} & \mathbf{0} & \mathbf{0} & \mathbf{\Psi}_{1,7} & \mathbf{\Psi}_{1,r}\\ \hdashline \mathbf{0} & \mathbf{I} & & & & & & \\ \mathbf{0} & & \mathbf{I} & & & & \mathbf{0} & \\ \mathbf{0} & & & \mathbf{I} & & & & \\ \mathbf{0} & & & & \mathbf{I} & & & \\ \mathbf{0} & & & & & \mathbf{I} & & \\ \mathbf{0} & & \mathbf{0} & & & & \mathbf{I} & \\ \mathbf{0} & & & & & & & \mathbf{I}\end{array}\right],$$

$$\mathbf{u}_g^{(1)}=\begin{bmatrix}\mathbf{0}\\ \hdashline \mathbf{u}_2\\ \mathbf{u}_3\\ \mathbf{u}_4\\ \mathbf{u}_5\\ \mathbf{u}_6\\ \mathbf{u}_7\\ \mathbf{u}_r\end{bmatrix},\quad \mathbf{F}_a^{(1)}=\begin{bmatrix}\mathbf{K}_1^{-1}\mathbf{F}_1\\ \hdashline \mathbf{0}\\ \mathbf{0}\\ \mathbf{0}\\ \mathbf{0}\\ \mathbf{0}\\ \mathbf{0}\\ \mathbf{0}\end{bmatrix}, \tag{12b}$$

where $\mathbf{C}_1$ is the 1st condensation matrix, $\mathbf{u}_g^{(1)}$ is the 1st condensed global displacement vector, and $\mathbf{F}_a^{(1)}$ is the 1st additional force vector.

Applying the relation $\mathbf{u}_g=\mathbf{C}_1\mathbf{u}_g^{(1)}+\mathbf{F}_a^{(1)}$ in Eq. (12a) to $\mathbf{K}_g\mathbf{u}_g=\mathbf{F}_g$ in Eq. (7), we can obtain the 1st condensed linear static equation as follows

$$\mathbf{K}_g^{(1)}\mathbf{u}_g^{(1)}=\mathbf{F}_g^{(1)}$$
$$\text{with}\quad \mathbf{K}_g^{(1)}=\mathbf{K}_g\mathbf{C}_1,\quad \mathbf{F}_g^{(1)}=\mathbf{F}_g-\mathbf{K}_g\mathbf{F}_a^{(1)}, \tag{13}$$

in which $\mathbf{K}_g^{(1)}$ and $\mathbf{F}_g^{(1)}$ are the 1st condensed global stiffness matrix and force vector, respectively.

Then, using $\mathbf{C}_1$ and $\mathbf{F}_a^{(1)}$ in Eq. (12b), the partitioned formulation for the 1st condensed linear static equation, $\mathbf{K}_g^{(1)}\mathbf{u}_g^{(1)}=\mathbf{F}_g^{(1)}$, is expressed as

$$\left[\begin{array}{c:ccccccc}\mathbf{0} & \mathbf{0} & \mathbf{0} & \mathbf{0} & \mathbf{0} & \mathbf{0} & \mathbf{0} & \mathbf{0}\\ \hdashline \mathbf{0} & \mathbf{K}_2 & \mathbf{K}_{2,3} & \mathbf{0} & \mathbf{0} & \mathbf{0} & \mathbf{K}_{2,7} & \mathbf{K}_{2,r}\\ \mathbf{0} & & \hat{\mathbf{K}}_3^{(1)} & \mathbf{0} & \mathbf{0} & \mathbf{0} & \hat{\mathbf{K}}_{3,7}^{(1)} & \hat{\mathbf{K}}_{3,r}^{(1)}\\ \mathbf{0} & & & \mathbf{K}_4 & \mathbf{0} & \mathbf{K}_{4,6} & \mathbf{K}_{4,7} & \mathbf{K}_{4,r}\\ \mathbf{0} & & & & \mathbf{K}_5 & \mathbf{K}_{5,6} & \mathbf{K}_{5,7} & \mathbf{K}_{5,r}\\ \mathbf{0} & & & & & \mathbf{K}_6 & \mathbf{K}_{6,7} & \mathbf{K}_{6,r}\\ \mathbf{0} & & sym. & & & & \hat{\mathbf{K}}_7^{(1)} & \hat{\mathbf{K}}_{7,r}^{(1)}\\ \mathbf{0} & & & & & & & \hat{\mathbf{K}}_r^{(1)}\end{array}\right]\begin{bmatrix}\mathbf{0}\\ \hdashline \mathbf{u}_2\\ \mathbf{u}_3\\ \mathbf{u}_4\\ \mathbf{u}_5\\ \mathbf{u}_6\\ \mathbf{u}_7\\ \mathbf{u}_r\end{bmatrix}=\begin{bmatrix}\mathbf{0}\\ \hdashline \mathbf{F}_2\\ \hat{\mathbf{F}}_3^{(1)}\\ \mathbf{F}_4\\ \mathbf{F}_5\\ \mathbf{F}_6\\ \hat{\mathbf{F}}_7^{(1)}\\ \hat{\mathbf{F}}_r^{(1)}\end{bmatrix}, \tag{14}$$

$$\hat{\mathbf{K}}_3^{(1)}=\mathbf{K}_3+\mathbf{K}_{1,3}^T\mathbf{\Psi}_{1,3},\quad \hat{\mathbf{K}}_{3,7}^{(1)}=\mathbf{K}_{3,7}+\mathbf{K}_{1,3}^T\mathbf{\Psi}_{1,7},$$
$$\hat{\mathbf{K}}_{3,r}^{(1)}=\mathbf{K}_{3,r}+\mathbf{K}_{1,3}^T\mathbf{\Psi}_{1,r}, \tag{15a}$$

$$\hat{\mathbf{K}}_7^{(1)}=\mathbf{K}_7+\mathbf{K}_{1,7}^T\mathbf{\Psi}_{1,7},\quad \hat{\mathbf{K}}_{7,r}^{(1)}=\mathbf{K}_{7,r}+\mathbf{K}_{1,7}^T\mathbf{\Psi}_{1,r},$$
$$\hat{\mathbf{K}}_r^{(1)}=\mathbf{K}_r+\mathbf{K}_{1,r}^T\mathbf{\Psi}_{1,r}, \tag{15b}$$

$$\hat{\mathbf{F}}_3^{(1)}=\mathbf{F}_3+\mathbf{\Psi}_{1,3}^T\mathbf{F}_1,\quad \hat{\mathbf{F}}_7^{(1)}=\mathbf{F}_7+\mathbf{\Psi}_{1,7}^T\mathbf{F}_1,$$
$$\hat{\mathbf{F}}_r^{(1)}=\mathbf{F}_r+\mathbf{\Psi}_{1,r}^T\mathbf{F}_1, \tag{15c}$$

where the hat ^ denotes the substructural terms to be updated during the condensation procedure. Note that the stiffness, displacement, and force terms corresponding to the 1st substructure become zero, and the stiffness and force terms corresponding to the ancestor substructural set for the 1st substructure, that is $A_1=\{3,7,r\}$, are only updated by the 1st condensation matrix $\mathbf{C}_1$.

In Eq. (14), the 2nd row equation is expressed as

$$\mathbf{K}_2\mathbf{u}_2+\mathbf{K}_{2,3}\mathbf{u}_3+\mathbf{K}_{2,7}\mathbf{u}_7+\mathbf{K}_{2,r}\mathbf{u}_r=\mathbf{F}_2, \tag{16}$$

and thus, the displacement vector $\mathbf{u}_2$ corresponding to the 2nd substructure is written by

$$\mathbf{u}_2=\mathbf{\Psi}_{2,3}\mathbf{u}_3+\mathbf{\Psi}_{2,7}\mathbf{u}_7+\mathbf{\Psi}_{2,r}\mathbf{u}_r+\mathbf{K}_2^{-1}\mathbf{F}_2, \tag{17a}$$

$$\mathbf{\Psi}_{2,3}=-\mathbf{K}_2^{-1}\mathbf{K}_{2,3},\quad \mathbf{\Psi}_{2,7}=-\mathbf{K}_2^{-1}\mathbf{K}_{2,7},\quad \mathbf{\Psi}_{2,r}=-\mathbf{K}_2^{-1}\mathbf{K}_{2,r}. \tag{17b}$$

Substituting $\mathbf{u}_2$ in Eq. (17) into $\mathbf{u}_g^{(1)}$ in Eq. (12b), the 1st condensed global displacement vector $\mathbf{u}_g^{(1)}$ can be rewritten as

$$\mathbf{u}_g^{(1)}=\mathbf{C}_2\mathbf{u}_g^{(2)}+\mathbf{F}_a^{(2)}, \tag{18a}$$

$$\mathbf{C}_2=\left[\begin{array}{cc|cccccc}
\mathbf{0}&\mathbf{0}&\mathbf{0}&\mathbf{0}&\mathbf{0}&\mathbf{0}&\mathbf{0}&\mathbf{0}\\
\mathbf{0}&\mathbf{0}&\mathbf{\Psi}_{2,3}&\mathbf{0}&\mathbf{0}&\mathbf{0}&\mathbf{\Psi}_{2,7}&\mathbf{\Psi}_{2,r}\\
\hline
\mathbf{0}&\mathbf{0}&\mathbf{I}&&&&&\\
\mathbf{0}&\mathbf{0}&&\mathbf{I}&&&\mathbf{0}&\\
\mathbf{0}&\mathbf{0}&&&\mathbf{I}&&&\\
\mathbf{0}&\mathbf{0}&&&&\mathbf{I}&&\\
\mathbf{0}&\mathbf{0}&&\mathbf{0}&&&\mathbf{I}&\\
\mathbf{0}&\mathbf{0}&&&&&&\mathbf{I}
\end{array}\right],$$

$$\mathbf{u}_g^{(2)}=\left[\begin{array}{c}\mathbf{0}\\ \mathbf{0}\\ \hline \mathbf{u}_3\\ \mathbf{u}_4\\ \mathbf{u}_5\\ \mathbf{u}_6\\ \mathbf{u}_7\\ \mathbf{u}_r\end{array}\right],\quad \mathbf{F}_a^{(2)}=\left[\begin{array}{c}\mathbf{0}\\ \mathbf{K}_2^{-1}\mathbf{F}_2\\ \hline \mathbf{0}\\ \mathbf{0}\\ \mathbf{0}\\ \mathbf{0}\\ \mathbf{0}\\ \mathbf{0}\end{array}\right], \tag{18b}$$

where $\mathbf{C}_2$, $\mathbf{u}_g^{(2)}$, and $\mathbf{F}_a^{(2)}$ are the 2nd condensation matrix, the 2nd condensed global displacement vector, and the 2nd additional force vector, respectively.

Then, using Eq. (18a) in Eq. (13), we can obtain the 2nd condensed linear static equation as follows

$$\begin{gathered}\mathbf{K}_g^{(2)}\mathbf{u}_g^{(2)}=\mathbf{F}_g^{(2)},\\ \text{with}\ \ \mathbf{K}_g^{(2)}=\mathbf{K}_g^{(1)}\mathbf{C}_2,\ \ \mathbf{F}_g^{(2)}=\mathbf{F}_g^{(1)}-\mathbf{K}_g^{(1)}\mathbf{F}_a^{(2)},\end{gathered} \tag{19}$$

in which $\mathbf{K}_g^{(2)}$ is the 2nd condensed global stiffness matrix, and $\mathbf{F}_g^{(2)}$ is the 2nd condensed global force vector.

From Eq. (18b) and Eq. (19), the following partitioned formulation for the 2nd condensed linear static equation $\mathbf{K}_g^{(2)}\mathbf{u}_g^{(2)}=\mathbf{F}_g^{(2)}$ is obtained

$$\left[\begin{array}{cc|cccccc}
\mathbf{0}&\mathbf{0}&\mathbf{0}&\mathbf{0}&\mathbf{0}&\mathbf{0}&\mathbf{0}&\mathbf{0}\\
\mathbf{0}&\mathbf{0}&\mathbf{0}&\mathbf{0}&\mathbf{0}&\mathbf{0}&\mathbf{0}&\mathbf{0}\\
\hline
\mathbf{0}&\mathbf{0}&\hat{\mathbf{K}}_3^{(2)}&\mathbf{0}&\mathbf{0}&\mathbf{0}&\hat{\mathbf{K}}_{3,7}^{(2)}&\hat{\mathbf{K}}_{3,r}^{(2)}\\
\mathbf{0}&\mathbf{0}&&\mathbf{K}_4&\mathbf{0}&\mathbf{K}_{4,6}&\mathbf{K}_{4,7}&\mathbf{K}_{4,r}\\
\mathbf{0}&\mathbf{0}&&&\mathbf{K}_5&\mathbf{K}_{5,6}&\mathbf{K}_{5,7}&\mathbf{K}_{5,r}\\
\mathbf{0}&\mathbf{0}&&&&\mathbf{K}_6&\mathbf{K}_{6,7}&\mathbf{K}_{6,r}\\
\mathbf{0}&\mathbf{0}&&sym.&&&\hat{\mathbf{K}}_7^{(2)}&\hat{\mathbf{K}}_{7,r}^{(2)}\\
\mathbf{0}&\mathbf{0}&&&&&&\hat{\mathbf{K}}_r^{(2)}
\end{array}\right]
\left[\begin{array}{c}\mathbf{0}\\ \mathbf{0}\\ \hline \mathbf{u}_3\\ \mathbf{u}_4\\ \mathbf{u}_5\\ \mathbf{u}_6\\ \mathbf{u}_7\\ \mathbf{u}_r\end{array}\right]=
\left[\begin{array}{c}\mathbf{0}\\ \mathbf{0}\\ \hline \hat{\mathbf{F}}_3^{(2)}\\ \mathbf{F}_4\\ \mathbf{F}_5\\ \mathbf{F}_6\\ \hat{\mathbf{F}}_7^{(2)}\\ \hat{\mathbf{F}}_r^{(2)}\end{array}\right], \tag{20}$$

and similarly as shown in Eq. (14), by the 2nd condensation matrix $\mathbf{C}_2$, all the terms corresponding to the 2nd substructure become zero, and the stiffness and force terms corresponding to the ancestor substructural set for the 2nd substructure, $A_2=\{3,7,r\}$, are updated as follows

$$\begin{gathered}\hat{\mathbf{K}}_3^{(2)}=\hat{\mathbf{K}}_3^{(1)}+\mathbf{K}_{2,3}^T\mathbf{\Psi}_{2,3},\ \ \hat{\mathbf{K}}_{3,7}^{(2)}=\hat{\mathbf{K}}_{3,7}^{(1)}+\mathbf{K}_{2,3}^T\mathbf{\Psi}_{2,7},\\ \hat{\mathbf{K}}_{3,r}^{(2)}=\hat{\mathbf{K}}_{3,r}^{(1)}+\mathbf{K}_{2,3}^T\mathbf{\Psi}_{2,r},\end{gathered} \tag{21a}$$

$$\begin{gathered}\hat{\mathbf{K}}_7^{(2)}=\hat{\mathbf{K}}_7^{(1)}+\mathbf{K}_{2,7}^T\mathbf{\Psi}_{2,7},\ \ \hat{\mathbf{K}}_{7,r}^{(2)}=\hat{\mathbf{K}}_{7,r}^{(1)}+\mathbf{K}_{2,7}^T\mathbf{\Psi}_{2,r},\\ \hat{\mathbf{K}}_r^{(2)}=\hat{\mathbf{K}}_r^{(1)}+\mathbf{K}_{2,r}^T\mathbf{\Psi}_{2,r}\end{gathered} \tag{21b}$$

$$\begin{gathered}\hat{\mathbf{F}}_3^{(2)}=\hat{\mathbf{F}}_3^{(1)}+\mathbf{\Psi}_{2,3}^T\mathbf{F}_2,\ \ \hat{\mathbf{F}}_7^{(2)}=\hat{\mathbf{F}}_7^{(1)}+\mathbf{\Psi}_{2,7}^T\mathbf{F}_2,\\ \hat{\mathbf{F}}_r^{(2)}=\hat{\mathbf{F}}_r^{(1)}+\mathbf{\Psi}_{2,r}^T\mathbf{F}_2.\end{gathered} \tag{21c}$$

In the same way, we can define the remaining 3rd through 7th condensation matrices ($\mathbf{C}_3$, $\mathbf{C}_4$, $\mathbf{C}_5$, $\mathbf{C}_6$, and $\mathbf{C}_7$); the 3rd through 7th condensed global displacement vectors ($\mathbf{u}_g^{(3)}$, $\mathbf{u}_g^{(4)}$, $\mathbf{u}_g^{(5)}$, $\mathbf{u}_g^{(6)}$, and $\mathbf{u}_g^{(7)}$); and the 3rd through 7th additional force vectors ($\mathbf{F}_a^{(3)}$, $\mathbf{F}_a^{(4)}$, $\mathbf{F}_a^{(5)}$, $\mathbf{F}_a^{(6)}$, and $\mathbf{F}_a^{(7)}$). Then, after all the remaining condensation procedures are carried out, we can obtain the fully condensed linear static equation.

The fully condensed linear static equation is expressed by

$$\mathbf{K}_g^{(7)}\mathbf{u}_g^{(7)}=\mathbf{F}_g^{(7)}, \tag{22}$$

where $\mathbf{K}_g^{(7)}$ and $\mathbf{F}_g^{(7)}$ are the final (=7th) condensed global stiffness matrix and force vector, respectively.

The partitioned formulation would be expressed as

$$\left[\begin{array}{ccccccc|c}
\mathbf{0}&\mathbf{0}&\mathbf{0}&\mathbf{0}&\mathbf{0}&\mathbf{0}&\mathbf{0}&\mathbf{0}\\
\mathbf{0}&\mathbf{0}&\mathbf{0}&\mathbf{0}&\mathbf{0}&\mathbf{0}&\mathbf{0}&\mathbf{0}\\
\mathbf{0}&\mathbf{0}&\mathbf{0}&\mathbf{0}&\mathbf{0}&\mathbf{0}&\mathbf{0}&\mathbf{0}\\
\mathbf{0}&\mathbf{0}&\mathbf{0}&\mathbf{0}&\mathbf{0}&\mathbf{0}&\mathbf{0}&\mathbf{0}\\
\mathbf{0}&\mathbf{0}&\mathbf{0}&\mathbf{0}&\mathbf{0}&\mathbf{0}&\mathbf{0}&\mathbf{0}\\
\mathbf{0}&\mathbf{0}&\mathbf{0}&\mathbf{0}&\mathbf{0}&\mathbf{0}&\mathbf{0}&\mathbf{0}\\
\mathbf{0}&\mathbf{0}&\mathbf{0}&\mathbf{0}&\mathbf{0}&\mathbf{0}&\mathbf{0}&\mathbf{0}\\
\hline
\mathbf{0}&\mathbf{0}&\mathbf{0}&\mathbf{0}&\mathbf{0}&\mathbf{0}&\mathbf{0}&\hat{\mathbf{K}}_r^{(7)}
\end{array}\right]
\left[\begin{array}{c}\mathbf{0}\\ \mathbf{0}\\ \mathbf{0}\\ \mathbf{0}\\ \mathbf{0}\\ \mathbf{0}\\ \mathbf{0}\\ \hline \mathbf{u}_r\end{array}\right]=
\left[\begin{array}{c}\mathbf{0}\\ \mathbf{0}\\ \mathbf{0}\\ \mathbf{0}\\ \mathbf{0}\\ \mathbf{0}\\ \mathbf{0}\\ \hline \hat{\mathbf{F}}_r^{(7)}\end{array}\right], \tag{23}$$

in which $\hat{\mathbf{K}}_r^{(7)}$, $\mathbf{u}_r$, and $\hat{\mathbf{F}}_r^{(7)}$ are the stiffness matrix, displacement vector, and force vector corresponding to the retained substructure, respectively. Note that, except for the terms related to the retained substructure, all the substructural terms become zero.

Finally, we can obtain the reduced linear static equation for the retained substructure

$$\hat{\mathbf{K}}_r^{(7)}\mathbf{u}_r=\hat{\mathbf{F}}_r^{(7)}, \tag{24}$$

and the displacement vector for the retained substructure, $\mathbf{u}_r$, is obtained by

$$\mathbf{u}_r=(\hat{\mathbf{K}}_r^{(7)})^{-1}\hat{\mathbf{F}}_r^{(7)}, \tag{25}$$

Because there is no approximation during the condensation procedures, the retained displacement vector $\mathbf{u}_r$ in Eq. (25) is mathematically the same as that calculated from the global model in Eq. (8).

Based on the derivation procedure described above, the updated stiffness and force terms during the condensation procedures can generally be described as follows

$$\hat{\mathbf{K}}_{j,k}^{(i)}=\hat{\mathbf{K}}_{j,k}^{(i-1)}+(\mathbf{K}_{i,j})^T\mathbf{\Psi}_{i,k} \tag{26a}$$

$$\text{with} \quad \boldsymbol{\Psi}_{i,k} = -\mathbf{K}_i^{-1}\mathbf{K}_{ik} \quad \text{for} \quad i \in B, \quad j,k \in A_i,$$

$$\hat{\mathbf{F}}_j^{(i)} = \hat{\mathbf{F}}_j^{(i-1)} + \boldsymbol{\Psi}_{i,j}^T \mathbf{F}_i \quad \text{for} \quad i \in B, \quad j \in A_i, \tag{26b}$$

$$\hat{\mathbf{K}}_{j,k}^{(0)} = \mathbf{K}_{j,k}, \quad \hat{\mathbf{F}}_j^{(0)} = \mathbf{F}_j, \tag{26c}$$

$$\hat{\mathbf{K}}_{j,k}^{(i)} = \hat{\mathbf{K}}_{j,k}^{(i-1)} + (\hat{\mathbf{K}}_{i,j}^{(i-1)})^T \boldsymbol{\Psi}_{i,k}$$
$$\text{with} \quad \boldsymbol{\Psi}_{i,k} = -(\hat{\mathbf{K}}_i^{(i-1)})^{-1}(\hat{\mathbf{K}}_{i,k}^{(i-1)}) \quad \text{for} \quad i \in H, \quad j,k \in A_i, \tag{26d}$$

$$\hat{\mathbf{F}}_j^{(i)} = \hat{\mathbf{F}}_j^{(i-1)} + \boldsymbol{\Psi}_{i,j}^T \hat{\mathbf{F}}_i^{(i-1)} \quad \text{for} \quad i \in H, \quad j \in A_i. \tag{26e}$$

The general formulation of the reduced linear static equation is written by

$$\hat{\mathbf{K}}_r^{(n)}\mathbf{u}_r = \hat{\mathbf{F}}_r^{(n)}, \tag{27}$$

where n is the number of the omitted substructures.

Finally, using Eq. (26), the stiffness matrix $\hat{\mathbf{K}}_r^{(n)}$ and the force vector $\hat{\mathbf{F}}_r^{(n)}$ for the retained substructure can be described as

$$\hat{\mathbf{K}}_r^{(n)} = \mathbf{K}_r + \sum_{i=1}^{n}(\hat{\mathbf{K}}_{i,r}^{(i-1)})^T \boldsymbol{\Psi}_{i,r}, \tag{28a}$$

$$\hat{\mathbf{F}}_r^{(n)} = \mathbf{F}_r + \sum_{i=1}^{n}\boldsymbol{\Psi}_{i,r}^T \hat{\mathbf{F}}_i^{(i-1)}. \tag{28b}$$

Note that, to calculate the stiffness matrix $\hat{\mathbf{K}}_r^{(n)}$ and force vector $\hat{\mathbf{F}}_r^{(n)}$ for the retained substructure, we have only to consider Eq. (26) and Eq. (28), which are very simple formulations represented by the submatrices. Therefore, we can efficiently construct the reduced linear static equation, $\hat{\mathbf{K}}_r^{(n)}\mathbf{u}_r = \hat{\mathbf{F}}_r^{(n)}$.

The computational procedure of the automated static condensation method proposed in this study is described in Fig. 3.

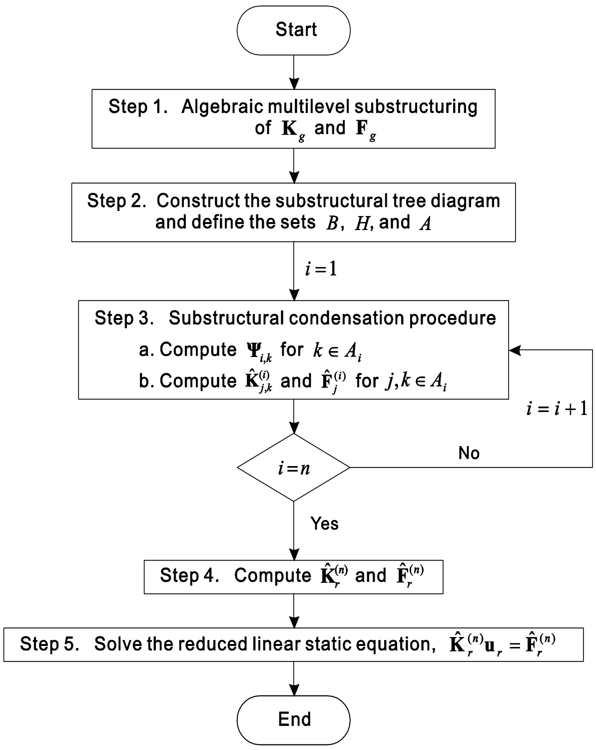

Fig. 3 Computational procedure of the automated static condensation method

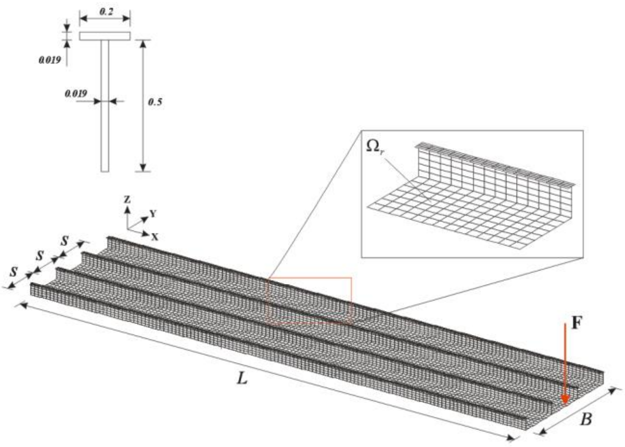

Fig. 4 Computational procedure of the automated static condensation method

4. Numerical examples

In this section, to evaluate the performance of the proposed method, we solve four practical structural problems (i.e., a stiffened plate, a jacket structure, a barge structure, and a spar structure). The numerical code is implemented with MATLAB, and a personal computer is used for computation (Intel core (TM) i7-3770, 3.40 GHz CPU, 32GB RAM).

To verify the solution accuracy of the proposed method, we compare the L_2-norm of the displacement vector $\mathbf{u}_r$ obtained from the reduced model, to that of the global model. The L_2-norm is defined as follows

$$\|\mathbf{u}_r\|_2 = \sqrt{\sum_i (\mathrm{u}_i^r)^2}, \tag{29}$$

where u_i^r denotes the i^{th} element in the displacement vector $\mathbf{u}_r$. We also investigate the computational cost of the proposed method, and compare to that of the original static condensation method, to show the computational efficiency of the proposed method.

All FE models are modeled using the MSC Patran, which is a very widely used commercial FE analysis software. We use a mild steel, so that Young's modulus E is 206 GPa, Poisson's ratio υ is 0.3, and density ρ is 7850 kg/m^3. For the algebraic multilevel substructuring, we use the METIS (Karypis and Kumar 1998) software package, which has frequently been used for efficient matrix reordering and partitioning.

Table 1 The L_2-norm of the displacement vector $\mathbf{u}_r$ obtained from the global and the reduced models for the stiffened plate problem

	Global model	Reduced model	
		Original static condensation	Proposed
L_2-norm	13.92	13.92	13.92

Table 2 Specific computational cost of the stiffened plate problem

Methods	Items	Related equations	Computation times	
			[sec]	Ratio [%]
Original static condensation	Calculation of $\mathbf{\Psi}$ matrix	3	286.74	99.87
	Calculation of $\overline{\mathbf{K}}$ matrix and $\overline{\mathbf{F}}$ vector	5	0.33	0.12
	Solving $\overline{\mathbf{K}}\mathbf{u}_r = \overline{\mathbf{F}}$	6	0.04	0.01
	Total	-	287.11	100.00
Proposed	Algebraic substructuring	8	0.77	0.27
	Calculation of $\mathbf{\Psi}_{i,k}$ matrices	26	2.44	0.85
	Calculation of $\hat{\mathbf{K}}_r^{(n)}$ matrix and $\hat{\mathbf{F}}_r^{(n)}$ vector	28	3.17	1.11
	Solving $\hat{\mathbf{K}}_r^{(n)}\mathbf{u}_r = \hat{\mathbf{F}}_r^{(n)}$	27	0.04	0.01
	Total	-	6.42	2.24

4.1 Stiffened plate problem

We consider a stiffened plate, which is an important structural unit of ships and offshore structures, as shown in Fig. 4. Its length L is 26.0 m, breadth B is 6.0 m, and the stiffener spacing is 2.0 m. The stiffener is represented by a vertical web of height 0.5 m, a flange of breadth 0.2 m, and thickness of 0.019 m. The global FE model is modeled using 8580 shell elements (Dvorkin and Bathe 1984, Lee and Bathe 2004, Lee *et al*. 2014), and the number of DOFs is 52662. The applied point load $\mathbf{F}$ is 150 N, and the stiffened plate is fully fixed at x=0.

Using algebraic multilevel substructuring (Karypis and Kumar 1998), the global model is automatically partitioned into the retained substructure Ω_r and 255 omitted substructures with 8 substructural levels. Here, the number of DOFs for the retained substructure Ω_r is 1248.

Table 1 shows the L_2-norm of the displacement vector $\mathbf{u}_r$ obtained from the global and the reduced models for the stiffened plate problem. Table 2 shows the specific computational cost, and comparison to the computation time required for the original static condensation method. The proposed method only requires 2.24% of the previous computation time. From the results, we can conclude that the proposed method outperforms the original static condensation method in computational efficiency without loss of accuracy.

4.2 Jacket structure problem

In Fig. 5, the jacket structure is considered. The height H and the width B are 87 m and 37 m, respectively, and the thickness is 0.025 m. We use 26484 shell elements for finite element modeling. The number of total DOFs is 155766. The applied point load $\mathbf{F}$ is 100 N, and the fixed boundary condition is imposed at z=0.

The retained substructure Ω_r is defined at the connection of the jacket structure where a fatigue crack could occur due to the geometrical discontinuity. The number of DOFs for the retained substructure is 6816. The global model is partitioned into one retained and 511 omitted substructures, and the substructural tree diagram is constructed with 9 substructural levels.

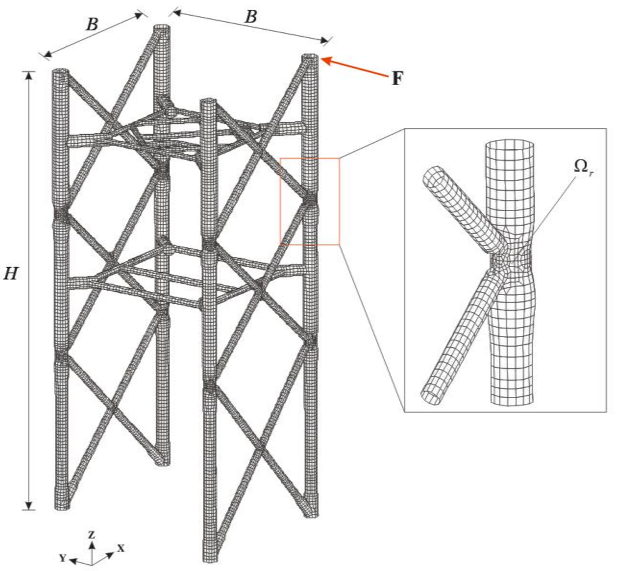

Fig. 5 Jacket structure problem (26484 shell elements, Global model of 155766 DOFs, Retained substructure Ω_r of 6816 DOFs)

Table 3 The L_2-norm of the displacement vector $\mathbf{u}_r$ obtained from the global and reduced models for the jacket structure problem

	Global model	Reduced model	
		Original static condensation	Proposed
L_2-norm	38.98	38.98	38.98

Table 3 presents the L_2-norm of the displacement vector $\mathbf{u}_r$ for the jacket structure problem, and it shows that the proposed method provides same accuracy as with the global analysis. The specific computational costs for the original static condensation and the proposed methods are described in Table 4. It is determined that the proposed method only requires 1.01% of the computation time needed for the original static condensation method. That is, the proposed method is about 100 times faster than the original static condensation method.

4.3 Barge structure problem

A barge structure is considered in Fig. 6. The length L, breadth B, height H, and draft D are 140.0 m, 37.0 m, 12.0 m, and 8.8 m, respectively.

Table 4 Specific computational cost for the jacket structure problem

Methods	Items	Related equations	Computation times [sec]	Computation times Ratio [%]
Original static condensation	Calculation of $\mathbf{\Psi}$ matrix	3	2048.41	99.87
	Calculation of $\overline{\mathbf{K}}$ matrix and $\overline{\mathbf{F}}$ vector	5	1.52	0.12
	Solving $\overline{\mathbf{K}}\mathbf{u}_r = \overline{\mathbf{F}}$	6	0.14	0.01
	Total	-	2050.07	100.00
Proposed	Algebraic substructuring	8	1.52	0.07
	Calculation of $\mathbf{\Psi}_{i,k}$ matrices	26	13.29	0.65
	Calculation of $\hat{\mathbf{K}}_r^{(n)}$ matrix and $\hat{\mathbf{F}}_r^{(n)}$ vector	28	5.71	0.28
	Solving $\hat{\mathbf{K}}_r^{(n)}\mathbf{u}_r = \hat{\mathbf{F}}_r^{(n)}$	27	0.14	0.01
	Total	-	20.66	1.01

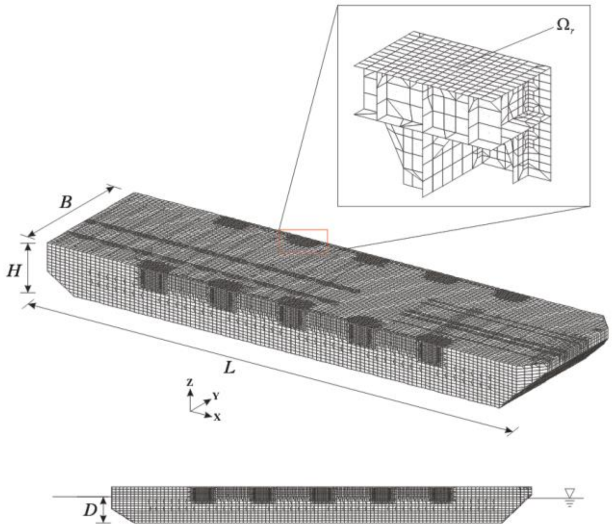

Fig. 6 Barge structure problem (123770 shell elements, Global model of 347604 DOFs, Retained substructure Ω_r of 5268 DOFs)

The FE model is constructed with 123770 shell elements, and the number of total DOFs is 347604. Hydrostatic pressure is applied, and the density of the sea is 1025 kg/m^3. The fixed boundary condition is imposed at the four corners on the bottom of the barge structure.

A part of the upper deck is defined as the retained substructure Ω_r, and its number of DOFs is 5268. To obtain a more accurate analysis result, the retained substructure Ω_r has a finer mesh than the other part. To construct the reduced model, the global stiffness matrix and force vectors are partitioned into 1023 omitted substructures with 10 substructural levels, using algebraic multilevel substructuring. From the numerical results described in Table 5 and Table 6, we can conclude that the proposed method can handle large FE models with excellent computational efficiency, compared to the original static condensation method.

Table 5 The L_2-norm of the displacement vector $\mathbf{u}_r$ obtained from the global and the reduced model for the barge structure problem

	Global model	Reduced model: Original static condensation	Reduced model: Proposed
L_2-norm	4.42	4.42	4.42

Table 6 Computational cost for the barge structure problem

Methods	Number of substructures omitted, n	Computation times [sec]	Computation times Ratio [%]
Original static condensation	-	8701.86	100.00
Proposed	512	332.14	3.81

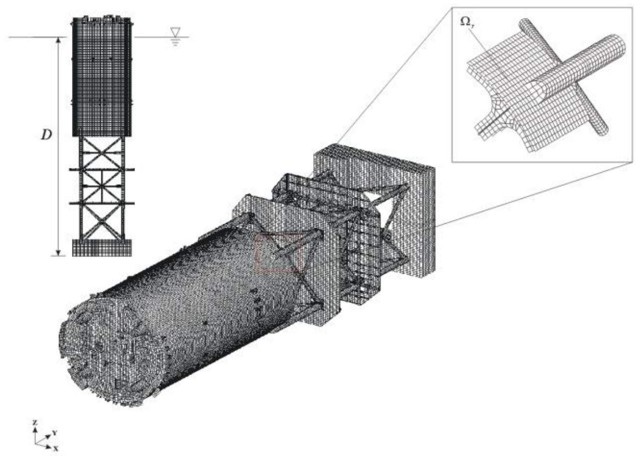

Fig. 7 Spar structure problem (337825 shell elements, Global model of 1831242 DOFs, Retained substructure Ω_r of 18084 DOFs)

4.4 Spar structure problem

Let us consider a spar structure such as shown in Fig. 7. The structure was modeled using 337825 shell finite elements, and the number of total DOFs is 1831242. The retained substructure Ω_r considered has 18084 DOFs. Hydrostatic pressure is applied, and the draft D and density of the sea are 190.0 m and 1025 kg/m^3, respectively.

For this FE model, the static condensation method could not construct a reduced model due to the large amount of computer memory required to store the constraint mode matrix $\mathbf{\Psi}$, which is an almost fully populated matrix. Using the proposed method, after defining the retained substructure Ω_r, the remaining part is partitioned into 4095 omitted substructures automatically, and the substructural tree diagram of 12 levels is constructed.

Table 7 The L_2-norm of the displacement vector $\mathbf{u}_r$ obtained from the global and reduced models for the spar structure problem

	Global model	Reduced model: Original static condensation	Reduced model: Proposed
L_2-norm	637.00	637.00	637.00

Table 8 Computational cost for the spar structure problem

Methods	Number of substructures omitted, n	Computation times [sec]
Original static condensation	-	N/A
Proposed	4095	6307.15

Table 7 and Table 8 present the accuracy and computational cost of the proposed method, respectively. We observed that the proposed method could provide reduced models with excellent computational efficiency for large FE models (over 10^6 DOFs).

5. Comparison with the superelement technique

In this section, we compare the computational efficiency of the proposed method with that of the superelement technique, which is a well-known reduction method embedded in MSC Nastran.

The superelement technique was originally proposed by applying the physical domain-based substructuring to the original static condensation method to reduce the computational cost for computing the constraint mode matrix $\mathbf{\Psi}$ described in Eq. (3).

However, with the superelement technique, when the number of the omitted substructures defined is small, each omitted substructure contains relatively large DOFs and the computational cost to construct the constraint mode matrix $\mathbf{\Psi}$ is still expensive. Furthermore, it requires huge modeling effort of substructuring to define the many omitted substructures (over 100 omitted substructures). That is, the superelement technique has an inefficiency for solving large FE models over 10^6 DOFs.

The major difference of the newly proposed method from the superelement technique comes from how to accomplish substructuring. With the superelement technique, the substructuring is accomplished manually using physical domain-based partitioning, and considering the geometry feature of the global structure. On the other hand, with the proposed method, the large number of omitted substructures are defined automatically in the algebraic perspective, and we only have to define the retained substructure Ω_r using the algebraic multilevel substructuring procedure as shown in Fig. 3. This feature is the most attractive strength of the proposed method, because there is no need for the demanding modeling effort of substructuring to define the omitted substructures as required with the superelement technique.

To compare the performance of the superelement technique and the proposed method, the spar structure problem in Fig. 7 is considered again. For the superelement technique, the spar structure is partitioned into 30 omitted substructures and the retained substructure Ω_r.

Table 9 shows the computational cost. Compared to the computation time required for the superelement technique, the proposed method requires only 20.49% of the computation time. Therefore, we can say that the proposed method is more competitive than the superelement technique regarding the aspect of computational efficiency.

Table 9 Comparison of computational costs for the superelement technique and the proposed method in the spar structure problem

Methods	Number of the substructures omitted, n	Computation times	
		[sec]	Ratio [%]
Superelement technique	30	17596.90	100.00
Proposed	4095	6307.15	20.49

6. Conclusions

In this study, we proposed the new automated static condensation method. Using the algebraic multilevel substructuring technique, the global FE model was partitioned into many substructures, and through matrix re-permutation considering the node numbers of the local model of interest, the retained substructure was defined. Then, the remaining substructures were automatically designated as the omitted substructures. The sequential condensation procedure was expressed as a way of updating the substructural matrices, and the general formulation of the reduced model was very efficiently expressed with submatrix operations that were easier to compute. To investigate the performance of the proposed method, the calculations for several large structural FE models were done, and the numerical results showed that the computational efficiency of the proposed method was much superior to that of the original static condensation method with the superelement technique.

In future work, the proposed method will be practically applied to a variety of structural analyses of large FE models requiring re-analyses, such as local analysis used to consider design modifications, local non-linear analysis, and local fatigue analysis considering a load history varying with time.

Acknowledgments

This research was financially supported by the Offshore Engineering Research Department of Hyundai Heavy Industries, and the Climate Change Research Hub of KAIST (Grant No. N01150026). The authors would like to thank Professor Phill-Seung Lee at KAIST for his special effort for this research.

References

Agrawal, O.P., Danhof, K.J. and Kumar, R. (1994), "A superelement model based parallel algorithm for vehicle dynamics", *Comput. Struct.*, **51**(4), 411-423.

Benfield, W.A. and Hruda R.F. (1971), "Vibration analysis of structures by component mode substitution", *AIAA J.*, **9**, 1255-1261.

Bennighof, J.K. and Lehoucq, R.B. (2004), "An automated multilevel substructuring method for eigenspace computation in linear elastodynamics", *SIAM J. Sci. Comput.*, **25**(6), 2084-2106.

Boo, S.H. and Lee, P.S. (2017), "A dynamic condensation method using algebraic substructuring", *Int. J. Numer. Meth. Eng.*, **109**(12), 1701-1720.

Boo, S.H., Kim, J.G. and Lee, P.S. (2016), "A simplified error estimator for the Craig-Bampton method and its application to error control", *Comput. Struct.*, **164,** 53-62.

Boo, S.H., Kim, J.G. and Lee, P.S. (2016), "Error estimation method for automated multi-level substructuring method", *Int. J. Numer. Meth. Eng.*, **106**, 927-950.

Cardona, A. (2000), "Superelements modelling in flexible multibody dynamics", *Multib. Syst. Dyn.*, **4**(2-3), 245-266

Craig, R.R. and Bampton M.C.C. (1968), "Coupling of substructures for dynamic analysis", *AIAA J.*, **6**(7), 1313-1319.

Dvorkin, E.N. and Bathe, K.J. (1984), "A continuum mechanics based four-node shell element for general nonlinear analysis", *Eng. Comput.*, **1**(1), 77-88.

Friswell, S.D., Garvey M.I. and Penny J. (1995), "Model reduction using dynamic and iterated IRS techniques", *J. Sound Vib.*, **186**(2), 311-323.

George, A. (1973), "Nested dissection of a rectangular finite element mesh", *SIAM J. Numer. Anal.*, **10**(2), 345-363.

Guyan, R. (1965), "Reduction of stiffness and mass matrices", *AIAA J.*, **3**(2), 380.

Han, J.S. (2014), "Krylov subspace-based model order reduction for Campbell diagram analysis of large-scale rotordynamic systems", *Struct. Eng. Mech.*, **50**(1), 19-36.

Irons, B.M. (1963), "Eigenvalue economisers in vibration problems", *J. R. Aeronaut. Soc.*, **67**, 526.

Jagadish, B.G., Anuj, P.S., Parampal, S.C. and Ranjan, G. (2007), "Free vibration analysis of rotating tapered blades using Fourier-p superelement", *Struct. Eng. Mech.*, **27**(2), 243-257.

Ju, F. and Choo, Y.S. (2005), "Super element approach to cable passing through multiple pulleys", *Int. J. Solid. Struct.*, **42**(11-12), 3533-3547.

Karypis, G. and Kumar, V. (1998), "METIS v4.0, A software package for partitioning unstructured graphs, partitioning meshes, and computing fill-reducing orderings of sparse matrices", Technical Report, University of Minnesota, Minneapolis, MN, USA.

Lee, P.S. and Bathe, K.J. (2004), "Development of MITC isotropic triangular shell finite elements", *Comput. Struct.*, **82**(11-12), 945-962.

Lee, Y.G., Lee, P.S. and Bathe, K.J. (2014), "The MITC3+ shell finite element and its performance", *Comput. Struct.*, **138**, 12-23.

Long, X., Yuan, W., Tan, K.H. and Lee, C.K. (2013), "A superelement formulation for efficient structural analysis in progressive collapse", *Struct. Eng. Mech.*, **48**(3), 309-331.

MacNeal, R.H. (1971), "Hybrid method of component mode synthesis", *Comput. Struct.*, **1**(4), 581-601.

MSC Nastran (2014), *Superelements User's Guide*, MSC Software Corporation, Newport Beach, CA, USA.

O'Callanhan, J. (1989), "A procedure for an improved reduced system (IRS) model", *Proceedings of the 7th International Modal Analysis Conference*, Las Vegas, USA, February.

Rubin, S. (1975), "Improved component-mode representation for structural dynamic analysis", *AIAA J.*, **13**(8), 995-1006.

Wilson, E.L. (1974), "The static condensation algorithm", *Int. J. Numer. Meth. Eng.*, **8**(1), 198-203.

Xia, Y. and Lin R. (2004), "A new iterative order reduction (IOR) method for eigensolutions of large structures", *Int. J. Numer. Meth. Eng.*, **59**, 153-172.

PL